International Journal of Pharmacology

ISSN 1811-7775

science alert

ansinet
Asian Network for Scientific Information

OPEN ACCESS International Journal of Pharmacology

ISSN 1811-7775
DOI: 10.3923/ijp.2021.271.280

Research Article
Inhibition of U87 Glioblastoma in BALB/c Nude Mice by Serenoa Repens Extract

Jie Li, Hui Lv, Yuqin Che and Jianhua Fan

Department of Neurology, The Fourth Affiliated Hospital of China Medical University, Shenyang 110032, People's Republic of China

Abstract

Background and Objective: Glioblastoma is the most common and invasive tumour in human and most glioma is malignant, grows rapidly with a high recurrence rate. This study aimed to study the anti-tumour effect and mechanism of *Serenoa repens* extract on glioblastoma in BALB/c nude mice. **Materials and Methods:** Mice were transplanted with U87 glioblastoma cells and assigned to four groups including blank, model, low-dose SR_{50} and high-dose SR_{300} groups. Survival test, tumour volume and weight were measured. Natural killer cell activity, spleen index and the $CD4^+/CD8^+$ ratio in spleen cells were assayed. Levels of NF-κB, Cox-2, MCP-1, Ang-1, annexin II, vimentin and RhoA were determined. **Results:** Compared to the model group, SR treatment resulted in significantly prolonged survival and a significantly reduced tumour volume and weight in a dose-dependent manner. The spleen index and NK cell activity were lower in the model group compared to that in the control group ($p<0.01$) and higher with high-dose SR treatment ($p<0.05$). Ratio of CD4+/CD8+ was increased after SR treatment with a dose-dependent ($p<0.05$). Level of NF-κB, COX-2, MCP-1, RhoA, annexin II and vimentin were significantly decreased, while Ang-1 level was significantly increased by SR treatment compared to the model group ($p<0.05$). **Conclusion:** SR could prolong survival and reduce tumour infiltration in U87 tumour-bearing mice by NF-κB/Cox-2 signalling.

Key words: Glioblastoma, angiogenesis, Chinese medicine, RhoA, serenoa repens, chemotherapy, rho-associated protein kinase

Citation: Li, J., H. Lv, Y. Che and J. Fan, 2021. Inhibition of U87 glioblastoma in BALB/c nude mice by serenoa repens extract. Int. J. Pharmacol., 17: 271-280.

Corresponding Author: Jianhua Fan, Department of Neurology, The Fourth Affiliated Hospital of China Medical University, Shenyang 110032, People's Republic of China

Copyright: © 2021 Jie Li *et al.* This is an open access article distributed under the terms of the creative commons attribution License, which permits unrestricted use, distribution and reproduction in any medium, provided the original author and source are credited.

Competing Interest: The authors have declared that no competing interest exists.

Data Availability: All relevant data are within the paper and its supporting information files.

INTRODUCTION

Glioblastoma is the most common and invasive tumour in human. And most glioma is malignant, grows rapidly with a high recurrence rate[1,2]. There is no good treatment for glioblastoma at present and patients suffered from short survival time and high mortality rate. Surgery, radiotherapy and chemotherapy are standard treatments, however, the high invasiveness of glioblastoma, the dose limitations of normal brain tissue and its effects on the blood-brain barrier result in an average survival time of only 18-21 months, with a 5 years survival rate between 20-30%[3]. There is therefore tremendous clinical relevance for studies that add to the understanding of glioblastoma development and identify noel treatments is evident.

The nuclear factor κB (NF-κB) signalling pathway and its related genes regulate diverse activities, including physiological and pathological cellular differentiation and proliferation immune-related inflammation, apoptosis, tumour cell adhesion and metastasis[4]. NF-κB activity is increased in glioblastoma and has been associated with both malignancy and reduced sensitivity to radiotherapy and chemotherapy[5]. Cyclooxygenase-2 (Cox-2) is a co-enzyme of peroxidase. In prostate tissue, Cox-2 is not only expressed under physiological conditions but is expressed following tissue injury, inflammation and in tumors[6]. In glioblastoma, Cox-2 expression inhibited positively correlated with both malignancy and prognosis[7]. Interestingly, the Cox-2 promoter contains two NF-κB binding sites for transcriptional activation[8], suggesting that the NF-κB/Cox-2 pathway and glioblastoma incidence, invasion and metastasis may be related.

Angiogenesis is also an important factor in glioblastoma progression[9]. The angiogenin most closely associated with glioblastoma is angiopoietin-2 (Ang-2), which is also associated with metastasis[10]. The expression of Ang-2 is upregulated by Cox-2[11]. Angiopoietin-1 (Ang-1) also acts as a vascular stabilizing factor in glioblastoma by decreasing vascular permeability. Furthermore, NF-κB regulates Ang-1-mediated inflammation[12,13].

The diffuse infiltration of glioblastoma tumour cells, which results in substantial metastasis is clinically challenging. Both tumour invasion and metastasis depend on cytoskeletal reorganization. Particularly, Rho A, a small GTPase member of the Rho protein family, promotes tumour cell migration by inducing cytoskeletal changes via the Rho-associated protein kinase (ROCK), a downstream protein kinase[14]. In some malignant cells, inhibition of RhoA activation indirectly blocks downstream activation of NF-κB[15,16]. Additionally, vimentin is a component of the glial cell cytoskeleton that is regulated by RhoA signalling. Vimentin is abnormally expressed in malignant lung, breast, prostate, ovarian and kidney tumour cells and is associated with local invasion and metastasis; it is also used as a prognosis index for these cancers. Vimentin content is higher in glioblastoma than in normal brain tissue, where it is significantly correlated with the level of differentiation of glioblastoma tissue and may be involved in glioblastoma invasiveness and metastasis[17,18]. Finally, a member of the annexin family, annexin II, also affects cytoskeletal remodelling by triggering Rho/ROCK signalling. Knocking out annexin II slows tumour progression by decreasing glioblastoma cell proliferation, invasion and angiogenesis and by increasing apoptosis[19-23]. In glioblastoma, the level of annexin II in tumour tissues is associated with the degree of malignancy[24].

Serenoa Repens (SR) extracts shown to inhibit growth and induce apoptosis in a variety of cancer cells, especially prostate cancer[25]. A previous study indicated that STAT3 signal transduction can inhibit human glioblastoma cell proliferation and promote tumour cell apoptosis[26].

In this research, the study mechanism of SR extract inhibited the growth of U87 glioblastoma cells in BALB/c nude mice was achieved. SR could treat glioblastoma according to NF-κB/Cox-2 and RhoA signalling which related to immune regulation, angiogenesis and tumour invasion.

MATERIALS AND METHODS

Study area: Part of this study was carried out in the Fourth Affiliated Hospital of China Medical University, Shenyang, China and the other part was carried out in Liaoning University of Traditional Chinese Medicine, Shenyang, China from June, 2018-October, 2019.

Animals: 130 BALB/c nude mice (20±2 g) were taken from Beijing Hua Fu Kang Biotechnology Co., Ltd. (Beijing, China). Mice were housed in a specific pathogen-free animal room at the Animal Center, Liaoning University of Traditional Chinese Medicine, (Shenyang, China). Experimental procedures were performed one week after mice had adjusted to laboratory conditions.

Establishment of the U87 cell tumor-bearing BALB/c nude mice model: The U87 human glioblastoma cell line (Shanghai Hui Ying Biotechnology Co., Ltd., Shanghai, China) was maintained using standard tissue culture methods[27] with minor modification. Two randomly chosen mice had intraperitoneally injected U87 cells with a suspension of 1×10^5 cells/mL. One week after injection, the thick, milky ascites that had formed were aspirated, diluted with sterile

saline and grown in cultures adjusted to 1×10^7 cells/mL. Cell viability was over 95%. A total of 100 randomly selected BALB/c nude mice were injected with U87 cell suspensions at 30°C in the axilla of the right anterior limb. Masses developed approximately 5 days after injection and tumour removal indicated the successful establishment of the model.

BALB/c mouse lymphocyte extraction: 30 BALB/c mice were anaesthetized by intraperitoneal injection of chloral hydrate (0.3 mL/10 g, 1%) and 1 mL of peripheral whole blood was collected through the tail vein and anticoagulated with heparin sodium. The blood lymphocytes were washed with PBS 3 times, followed by resuspension in PBS buffer. Cell concentration was adjusted to 2×10^6 cells/mL for further use.

Animal allocation and treatment: Ten BALB/c nude mice were selected as the blank group. Sixty mice with tumours of similar mass were selected as the experimental group. Mice in the experimental group were randomly allocated into three groups including a model group (n = 20) which were given 10 mg kg^{-1} saline daily, a low-dose SR group (SR_{50}, n = 20) given 50 mg kg^{-1} SR extract daily and a high-dose SR group (SR_{300}, n = 20) given 300 mg kg^{-1} SR extract daily. SR extract or saline were administered orally every day for 4 weeks. All the mice were weighed daily. Ten mice were selected from each of the three treatment groups for survival estimations for an observation period of 50 days. The remaining were sacrificed 24 hrs after the last administration of saline or SR and axillary tumour tissues were removed for further study after 12 hrs rapidly.

Tumour inhibition by SR extract: Tumors were completely resected and the maximum and minimum diameters were measured with a millimetre calliper. Tumour volume (mm^3) was calculated as follows, after blotting with filter paper, Tumours Inhibition (TI) were calculated:

$$\text{Volume} = [\pi/6\times(\text{maximum diameter}+\text{minimum diameter})/2]^3$$

Immune function analysis: Another 30 tumour-bearing U87 BALB/c nude mice with similar tumour size were randomly divided into a model group, low-dose SR group (SR50) and high-dose SR group (SR300), respectively (n = 10). Before the intervention factor was applied, each nude mouse was injected with 0.5 mL of BALB/c mouse-derived lymphocyte suspension via the tail vein, followed by the corresponding drug intervention. Nude mice were killed 24 hrs after the last administration and the spleen was then taken and spleen index (mg g^{-1}) was calculated.

NK cell activity assay: Effector cell preparations were made after spleen removal for the assay of NK cell activity by lactate dehydrogenase (LDH) release. Spleen cell suspensions with over 95% viable cells were prepared by conventional methods and the concentration was adjusted to 2×10^7 cells/mL in RPMI 1640 medium (Beijing Hyclone Biotechnology Co. Ltd, Beijing, China).

YAC-1 target cells that had been cryopreserved at the Biotechnology Laboratory of Liaoning University of Traditional Chinese Medicine were sub-cultured for 24 hrs before use and the cell concentration was adjusted to 4×10^5 cells/mL in RPMI1640 medium. NK cell activity was assayed in 100 µL aliquots of target cells and effector cells (at a target ratio of 50:1) were added to U-shaped 96-well culture plates. The maximum target cell release was seen with 100 µL of target cell suspension and with 2.5% Triton. The assays were conducted in triplicates under 37°C and 5% CO_2 culture conditions for 4 hrs. The 96-well plates were then centrifuged at 1500 rpm for 5 min. Subsequently, 100 µL of clear supernatant from each well was pipetted into the well of a flat-bottom 96-well culture plate. 100 µL of LDH matrix liquid was added into each well. The reaction was allowed to continue for 3 min before adding 30 µL of 1 moL L^{-1} HCl and the optical density was measured at 490 nm. NK cell activity was calculated as a percentage as follows:

$CD4^+/CD8^+$ assay by flow cytometry: Spleen cell suspensions were prepared and filtered through a 200-mesh filter. The red blood cell lysate was analyzed and centrifuged at 1000 rpm for 5 min followed by washing with PBS solution. The supernatant was discarded and cells were resuspended in 1 mL of PBS and the concentration was adjusted to 10^5 cells/ mL using a cell-counting plate. 500 µL of adjusted cell suspension containing 5 µL of CD4-FITC/CD8-PE double-labelled antibody was added into a flow test tube, which was then incubated at room temperature for 20 min in dark. The incubated suspension was centrifuged at 1000 r/min for 5 min and the supernatant was discarded, followed by the addition of 0.5 mL of PBS solution to resuspend the cells. The expression of CD4/CD8 was then analyzed by flow cytometry. Up to 100,000 lymphocytes were collected for analysis. Per the lymphocyte FSC-SSC, the percentage of FITC single-positive cells, PE single-positive cells and FITC/PE double-positive cells were analyzed, respectively.

Western blot analysis: Tumor tissues collected from BALB/c nude mice were homogenized in 300 µL lysate buffer and centrifuged for 1 hr. The supernatant was saved for western blot assays and the concentration of total protein isolates was determined using a Bradford assay. Protein concentration was

then adjusted. The proteins were separated by sodium dodecyl sulfate-polyacrylamide gel electrophoresis (SDS-PAGE), transferred to polyvinylidene difluoride membranes and then blocked with 5% skim milk for 1 hr at room temperature. Primary antibodies, rabbit anti-human COX-2 polyclonal antibody, rabbit anti-human MCP-1 polyclonal antibody, anti-human annexin II polyclonal antibody, rabbit anti-human vimentin monoclonal antibody, rabbit anti-human-RhoA polyclonal antibody, rabbit anti-human NF-κB, rabbit anti-human-Ang-1 polyclonal antibody and rabbit anti-β actin antibody (all used at a concentration of 1:500; all from Santa Cruz, USA) were added sequentially and incubated overnight at 4°C. Then, membranes were washed with Tris-buffered saline Tween-20 (TBST) and incubated with horseradish peroxidase-conjugated secondary antibodies (Abcam, Cambridge, UK) at room temperature for 1 hr. The membranes were then washed three times with TBST and the signal was revealed using an enhanced chemiluminescence system, following the kit manufacturer's instructions. The samples were exposed to X-rays to obtain the grey values and the absorbance of each band was read with a Kodak Digital Science 130 analyzer (Kodak, Rochester, NY, USA). Finally, β-actin was used as an internal reference to calculate relative protein expression as the sample grey value/internal reference grey value.

Statistical analysis: SPSS 19.0 and GraphPad prism V5.01 were used for statistical analyses. Results were expressed as the Mean±standard deviation. Survival curves were calculated using the Kaplan-Meier method and the log-rank method was used to compare between-group differences in overall survival. Other indicators were compared by analysis of variance. Data with homogeneous variance were analyzed by the least significant differences method; otherwise, a Dunnett's test was used. A p-value<0.05 indicated a significant difference.

RESULTS

Survival and body weight of tumour-bearing BALB/c nude mice: Survival was significantly longer in the SR-treated groups (SR_{50}: 46.10±4.606 and SR_{300}: 47.60±3.534 days) than that in the model group (39.50±2.173 days, p<0.05). The SR of the two-dose groups didn't exhibit a significant effect on survival (p>0.05, Fig. 1a). The average body weight of the model group (19.30±0.857 g) was significantly lower than that of the blank group (23.02±2.463 g, p<0.01). Average body weight was significantly higher in the SR treatment groups (SR_{50}: 21.21±1.451 and SR_{300}: 21.90±1.049 g) compared with that of the model group (p<0.05). The SR dose had no significant effect on body weight (p>0.05, Fig. 1b).

Results indicated the changes in body weight in each BALB/c mouse study group. The p<0.05, blank vs. model group; p<0.05, SR treatment groups vs. model group; p>0.05, high vs. low-dose SR.

Tumour inhibition of BALB/c nude mice by SR extract: As shown in Fig. 2a, solid tumours were pale and fish-flesh in appearance without a notable capsule. Tumours were rich in blood vessels. The tumour volume was reduced in the SR-treated groups and was most significantly reduced in the high-dose group. In the model group, the tumour volume was 954.68±134.896 mm^3 and the weight was 1.21±0.164 g. In the low-dose (SR_{50}) group, the tumour volume was 721.23±128.705 mm^3 and the mean weight was 0.80±0.037 g. In the high-dose (SR_{300}) group, the tumour volume was 449.89±164.735 mm^3 and the tumour weight was 0.69±1.048 g. The tumour volumes and weights of both SR groups were significantly reduced compared to the model group (p<0.05). The difference in the tumour volumes of the high and low-dose groups was significant (p<0.05), but the

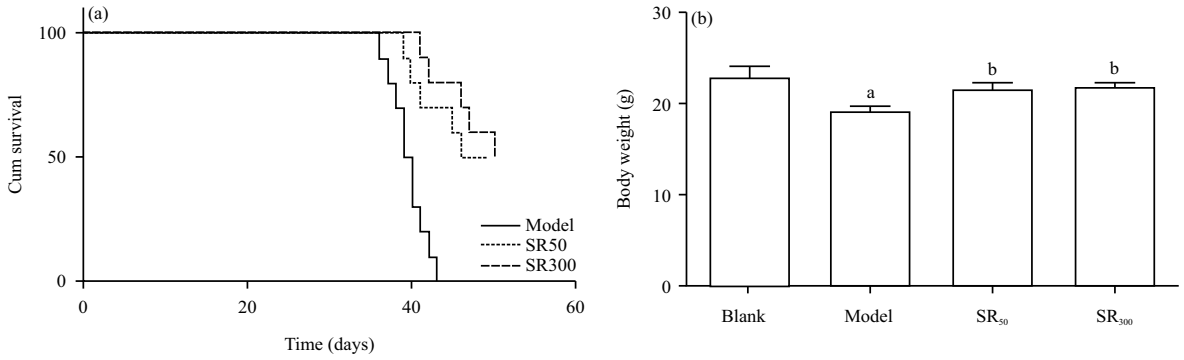

Fig. 1(a-b): (a) Mice survival curves and (b) body weight of BALB/c tumour bearing mice

Body weight of BALB/c mice in each treatment group, blank control vs. model group (^{a}p<0.05), SR treatment group vs. model group (^{b}p<0.05)

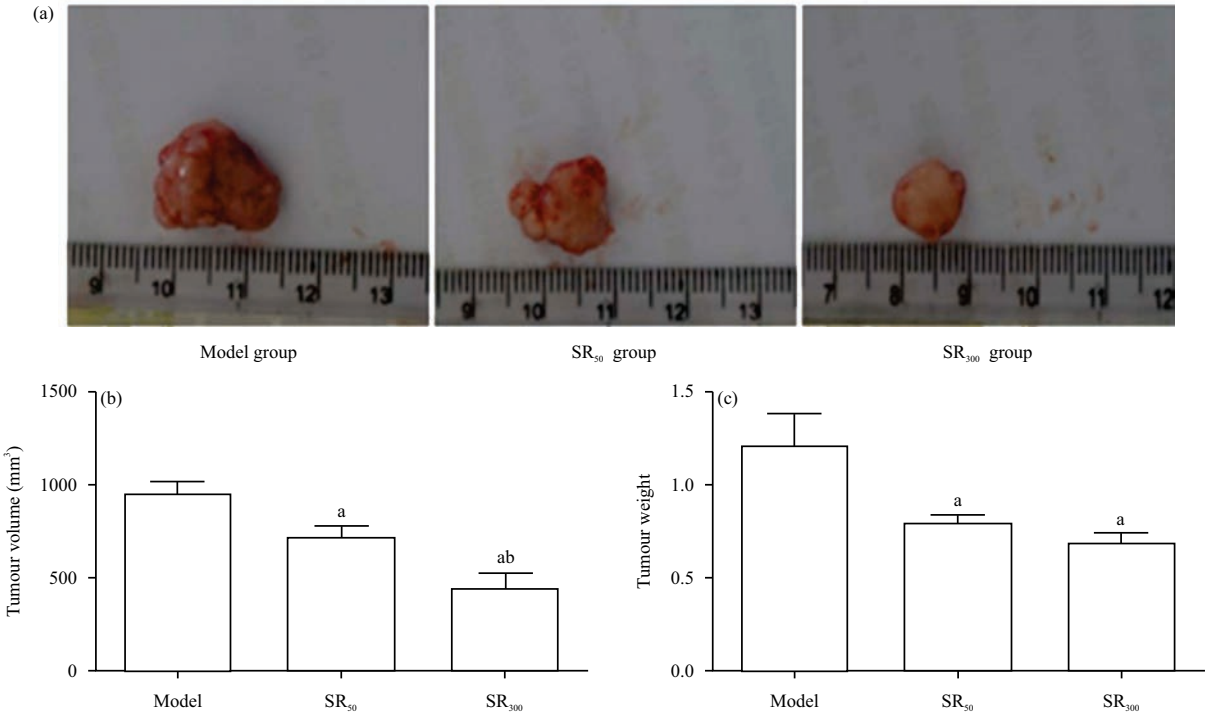

Fig. 2(a-c): Tumor inhibition of BALB/c nude mice by SR extract

(a) Solid tumours, (b) Tumour volume and (c) Weight of admiration groups. The tumour volume and weight of BALB/c mice in each treatment group, SR treatment group vs. model group ($^{a}p<0.05$), high-dose SR vs. low-dose SR ($^{b}p<0.05$)

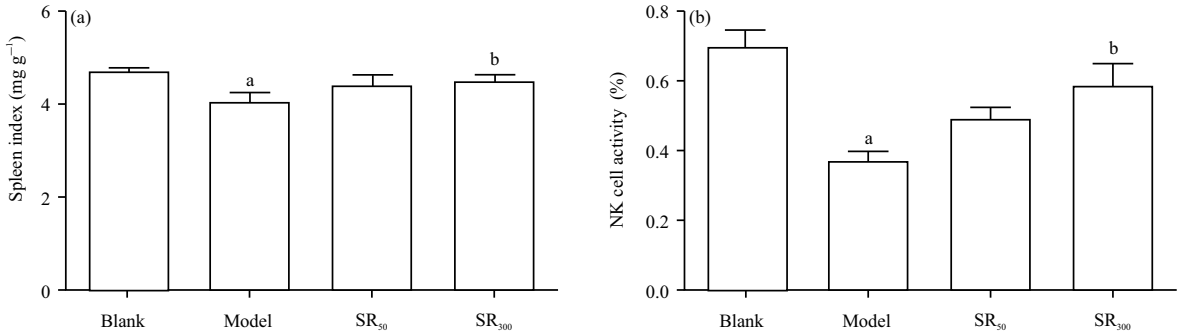

Fig. 3(a-b): (a) Spleen index and (b) NK cell activity

Spleen index and NK-cell activity of BALB/c mice in each treatment group, blank control vs. model group ($^{a}p<0.05$), high-dose SR vs. model group ($^{b}p<0.05$)

difference in tumour weight was not ($p>0.05$). Tumour inhibition rates were 33.88% in the low-dose group and 42.98% in the high-dose group (Fig. 2b-c).

Spleen index, NK cell activity and $CD4^{+}/CD8^{+}$ assay: The spleen index and NK cell activity were significantly lower in the model group than that in the blank group ($p<0.05$) and were significantly higher in the high-dose SR group than that in the model group ($p<0.05$). The differences between the low-dose SR and the model groups or between the high and low-dose groups were not significant ($p>0.05$, Fig. 3a-b). Flow cytometry assay indicated that the apoptotic rate of SR group was significantly lower than that of model group and approached the blank group (Fig. 4a). $CD4^{+}$ cells were significantly less numerous in the model group than in the blank group ($p<0.05$) and were significantly increased by high-dose SR ($p<0.05$). The number of $CD8^{+}$ cells was significantly higher in the model group than that in the blank group ($p<0.05$) and was decreased significantly following SR treatment. The numbers of $CD8^{+}$ cells in the two

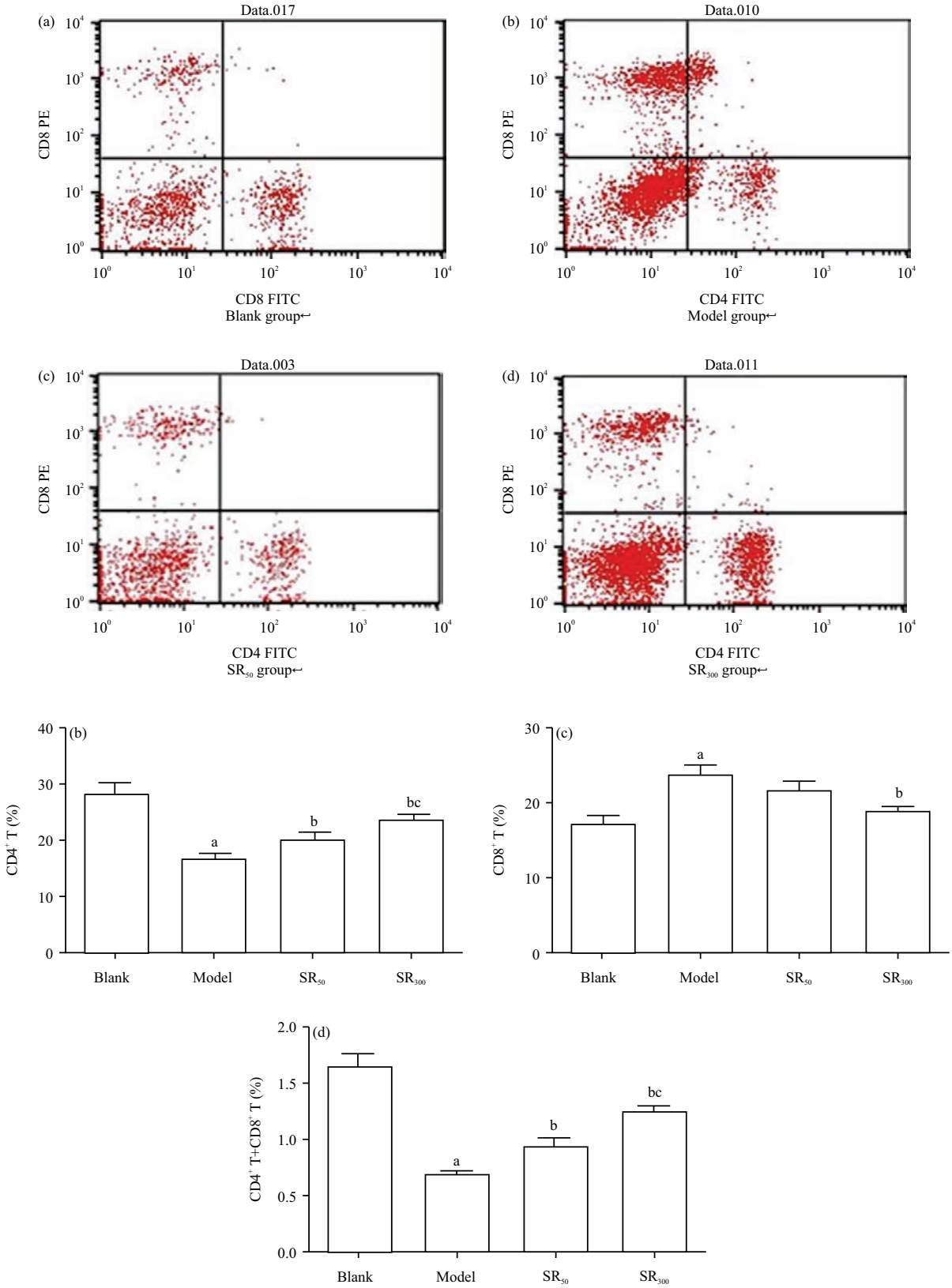

Fig. 4(a-d): (a) $CD4^+/CD8^+$ assay by flow cytometry, (b) $CD4^+$ cells, (c) CD8+cells and (d) $CD4^+/CD8^+$

[a]$p<0.05$, blank control vs. model group. [b]$p<0.05$ high-dose SR vs. model group. [c]$p<0.05$ high-dose SR vs. low-dose SR

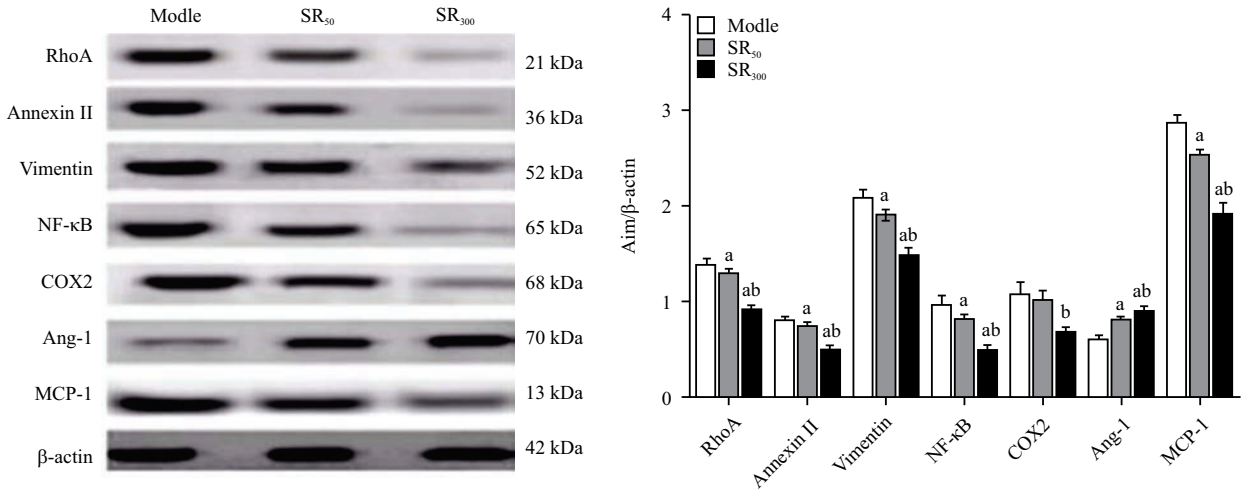

Fig. 5: Western blot of RhoA, annexin II, vimentin, NF-κB, Cox-2, Ang-1 and MCP-1 proteins relative to a β-actin reference
[a]p<0.05, SR groups vs. reference. [b]p<0.05 high-dose SR vs. low-dose SR

SR groups were not significantly different (p>0.05). The $CD4^+/CD8^+$ ratio was thus significantly increased by SR treatment (p<0.05, Fig. 4b-d).

RhoA, annexin II, vimentin, NF-κB, Cox-2, Ang-1 and MCP-1 expression in tumour-bearing BALB/c nude mice: The protein expression levels of tumour-bearing model and SR-treated nude mice were shown in Fig. 5. The expression of RhoA, annexin II, vimentin, NF-κB and MCP-1 protein was significantly decreased following SR treatment compared to that of model mice. Ang-1 protein expression, however, was significantly increased (p<0.01). Cox-2 protein expression was decreased after SR treatment, but the expression in the low-dose and model groups did not significantly differ (p>0.05). Cox-2 expression was significantly lower in that of the high-dose SR group than in the model group (p<0.01). Expression of all assayed proteins was significantly different between the high- and low-dose SR groups (p<0.01).

DISCUSSION

In this study, both high- and low-dose SR significantly prolonged the survival of glioblastoma tumour-bearing BALB/c nude mice. The tumour inhibition rates were 33.88% for low-dose SR treatment and 42.98% for high-dose SR treatment. SR inhibited glioblastoma cell growth and prolonged survival time. SR is widely used to treat benign prostatic hyperplasia and its associated lower urinary tract symptoms[28]. Recent studies have found that SR both inhibits the growth and induces apoptosis of cancer cells, including prostate cancer[25] and human glioblastoma cells *in vitro*[26,29].

The effects of SR on immune function, tumour cell invasion and tumour angiogenesis in tumour-bearing BALB/c nude mice were also investigated. Glioblastomas usually evade immune responses as well as $CD4^+/CD8^+$ and NK cells, which are a subset of lymphocytes with important roles in tumour immunity[30]. Compared to blank control mice, tumour-bearing mice had significantly lower $CD4^+$ cell numbers, significantly higher $CD8^+$ cell numbers and significantly decreased NK cell activity. The $CD4^+/CD8^+$ ratio was thus significantly decreased. $CD4^+$ activity in the nude mouse tumour cells increased with increased SR dose, but no obvious correlations in the number of $CD8^+$ numbers and activity of NK cell with the dose of SR. We believe that the immunological activity of SR involved regulating the response of multiple lymphocyte subsets to the presence of glioblastoma cells.

MCP-1 induces chemotaxis of monocytes, T lymphocytes and NK cells[31]. Correspondingly, the introduction of glioma cells transfected with MCP-1 into rat brains has been shown to increase tumour invasiveness[32]. In glioblastoma mice, an MCP-1 antibody has been shown to inhibit the infiltration of small glioblastoma cells and macrophages and prolong survival[33]. In this study, MCP-1 expression was significantly decreased after SR treatment and its expression was positively correlated with tumour volume reduction and prolongation of survival. It is therefore likely that MCP-1 is also involved in the observed anti-tumour effect of SR.

NF-κB, which acts upstream of MCP-1, is a regulator of cell survival, inflammation and immunity. In tumour cells, cytokines promote the activation of arachidonic acid metabolism and NF-κB by macrophages, resulting in further

promote increases in Cox-2 expression, ultimately leading to tumour invasion and metastasis. In this study, NF-κB and Cox-2 level in tumour-bearing nude mice was relatively high and the level of both proteins was decreased following SR treatment, in a dose-dependent manner. High Cox-2 expression accompanied by macrophage activation leads to the production of Prostaglandin E2 (PGE2) through the catalysis of arachidonic acid. PGE2 inhibits T and B lymphocyte-mediated antitumor responses and NK cell activity, resulting in the development of local tumour immunosuppression[34,35]. In prostate cancer models, SR has shown anti-tumour activity, resulting in down-regulated expression of inflammation-related genes in prostate tissue[36]. Reported indicated that SR could inhibit monocyte and T-cell infiltration one *in vitro*. And it also could induce apoptosis in androgen-dependent LNCaP prostate cancer cells by activating NF-κB signalling and reducing Cox-2 expression[36-38]. In this study, SR increased the $CD4^+/CD8^+$ ratio, increased NK cell activity, modulated immune functions and reduced MCP-1 expression by modulating NF-κB/Cox-2 signalling, ultimately inhibiting tumour progression.

Angiogenesis is a key step in the development and progression of glioblastoma. Ang-1 and Ang-2 are both active in this complex process. Ang-2 acts by promoting Vascular Endothelial Growth Factor (VEGF) activity and tumour growth. VEGF is expressed in both glioblastoma and vascular endothelial cells and its expression has been found to increase with increased glioblastoma stage[13,14]. The relationship between Ang-1 and tumour angiogenesis is still unclear, however, most studies indicate that Ang-1 and Ang-2 have opposing functions, with Ang-1 slowing tumour growth and Ang-2 promoting tumour progression. NF-κB signalling is involved in the regulation of Ang-1-mediated inflammation and Cox-2 up-regulates Ang-2 expression[15-17]. In this study, Ang-1 expression was higher in SR-treated mice than in model mice, but both NF-κB and Cox-2 expression decreased. In the present study, SR appears to have inhibited tumour angiogenesis and exerted anti-tumour effects *in vivo* by regulating the expression of Ang-1 and by inhibiting NF-κB/Cox-2 signalling.

Tumour cell invasion and metastasis are often closely associated with cytoskeletal changes and this is true for Glioblastoma. Rho A is a member of the Rho family of proteins and increased RhoA activity alters the structure of the cytoskeleton and promotes tumour cell migration. Vimentin is a component of the glial cell cytoskeleton that is regulated by RhoA signalling. Vimentin expression is significantly higher in glioblastoma than in normal brain tissue and its elevated expression is associated with the pathological differentiation of glioblastoma tissue and glioblastoma cell invasion and metastasis[22,23]. Additionally, annexin II is involved in cytoskeletal rearrangement, the opening of ion channels, fibrinolysis, endocytosis and exocytosis. It is highly expressed in glioblastoma cells and is associated with tumour angiogenesis, invasion and cell migration. Annexin II activity is regulated by the RhoA signalling pathway during intestinal epithelial cell migration[30]. In this study, RhoA, annexin II and vimentin expression in tumor tissue was significantly decreased after SR treatment (Fig. 5). SR might therefore have inhibited glioblastoma cell invasion and metastasis in tumour-bearing nude mice by blocking vimentin and annexin II expression via the RhoA signal transduction pathway. Some studies showed a similar tendency of RhoA and NF-κB expression in malignant tumour cells and have demonstrated that the inhibition of RhoA activation is indirectly blocked by NF-κB activation. RhoA is therefore likely to be an upstream factor of NF-κB.

CONCLUSION

Serenoa Repens extracts could inhibit the growth of U87 glioblastoma in BALB/c nude mice, possibly through the NF-κB/Cox-2 and RhoA signalling pathways. SR influenced immune responses, angiogenesis and tumour invasion. These results provide a rationale for further investigation of SR extracts in the clinical treatment of glioblastoma.

SIGNIFICANCE STATEMENT

This study revealed the importance and mechanism of *Serenoa Repens* extract (SR) in treating glioblastoma in BALB/c nude mice. It showed that SR could prolong survival and reduce tumour infiltration in U87 tumour-bearing mice by NF-κB/Cox-2 signalling. This study provides a new idea for the treatment of glioma and contributes to the development of clinical treatment of glioblastoma.

ACKNOWLEDGMENT

The present study was supported by the Natural Science Foundation of Liaoning Province of China (2019-ZD-0740).

REFERENCES

1. Wirsching, H.G., E. Galanis and M. Weller, 2016. Glioblastoma. Handb. Clin. Neurol., 134: 381-397.
2. Davis, M.E., 2016. Glioblastoma: Overview of disease and treatment. Clin. J. Oncol. Nurs., 20: S2-S8.

3. Bovenberg, M.S.S., M.H. Degeling and B.A. Tannous, 2013. Advances in stem cell therapy against gliomas. Trends Mol. Med., 19: 281-291.
4. Zhang, Q., M.J. Lenardo and D. Baltimore, 2017. 30 years of NF-κB: A blossoming of relevance to human pathobiology. Cell, 168: 37-57.
5. Friedmann-Morvinski, D., R. Narasimamurthy, Y. Xia, C. Myskiw, Y. Soda and I.M. Verma, 2016. Targeting NF-κB in glioblastoma: A therapeutic approach. Sci. Adv., Vol. 2. 10.1126/sciadv.1501292.
6. Desai, S.J., B. Prickril and A. Rasooly, 2018. Mechanisms of phytonutrient modulation of cyclooxygenase-2 (COX-2) and inflammation related to cancer. Nutr. Cancer, 70: 350-375.
7. Qiu, J., Z. Shi and J. Jiang, 2017. Cyclooxygenase-2 in glioblastoma multiforme. Drug Discovery Today, 22: 148-156.
8. Kim, J.H., H.K. Na, Y.K. Pak, Y.S. Lee, S.J. Lee, A. Moon and Y.J. Surh, 2008. Roles of ERK and p38 mitogen-activated protein kinases in phorbol ester-induced NF-κB activation and COX-2 expression in human breast epithelial cells. Chem. Biol. Interact., 171: 133-141.
9. Hundsberger, T., D.A. Reardon and P.Y. Wen, 2017. Angiogenesis inhibitors in tackling recurrent glioblastoma. Expert Rev. Anticancer Ther., 17: 507-515.
10. Peterson, T.E., N.D. Kirkpatrick, Y. Huang, C.T. Farrar and K.A. Marijt *et al*., 2016. Dual inhibition of Ang-2 and VEGF receptors normalizes tumor vasculature and prolongs survival in glioblastoma by altering macrophages. Proc. Nat. Acad. Sci. USA, 113: 4470-4475.
11. Tanaka, S., J.R. Wands and S. Arii, 2006. Induction of angiopoietin-2 gene expression by COX-2: A novel role for COX-2 inhibitors during hepatocarcinogenesis. J. Hepatol., 44: 233-235.
12. Tadros, A., D.P. Hughes, B.J. Dunmore and N.P.J. Brindle, 2003. ABIN-2 protects endothelial cells from death and has a role in the antiapoptotic effect of angiopoietin-1. Blood, 102: 4407-4409.
13. Hughes, D.P., M.B. Marron and N.P.J. Brindle, 2003. The antiinflammatory endothelial tyrosine kinase Tie2 interacts with a novel nuclear factor-κB inhibitor ABIN-2. Circ. Res., 92: 630-636.
14. Ridley, A.J., 2015. Rho GTPase signalling in cell migration. Curr. Opin. Cell Biol., 36: 103-112.
15. Cho, S.G., D. Li, L.J. Stafford, J. Luo, M. Rodriguez-Villanueva, Y. Wang and M. Liu, 2009. KiSS1 suppresses TNFα-induced breast cancer cell invasion via an inhibition of RhoA-mediated NF-κB activation. J. Cell. Biochem., 107: 1139-1149.
16. Cowell, C.F., I.K. Yan, T. Eiseler, A.C. Leightner, H. Döppler and P. Storz, 2009. Loss of cell-cell contacts induces NF-κB via RhoA-mediated activation of protein kinase D1. J. Cell. Biochem., 106: 714-728.
17. Murakami, M., K. Imabayashi, A. Watanabe, N. Takeuchi and R. Ishizaka *et al*., 2012. Identification of novel function of vimentin for quality standard for regenerated pulp tissue. J. Endodontics, 38: 920-926.
18. Satelli, A. and S. Li, 2011. Vimentin in cancer and its potential as a molecular target for cancer therapy. Cell. Mol. Life Sci., 68: 3033-3046.
19. Gurluler, E., O.S. Guner, L.V. Tumay, N.T. Kucukmetin, B. Hizli and A. Zorluoglu, 2014. Serum annexin A2 levels in patients with colon cancer in comparison to healthy controls and in relation to tumor pathology. Med. Sci. Monit., 20: 1801-1807.
20. Chaudhary, P., S.I. Thamake, P. Shetty and J.K. Vishwanatha, 2014. Inhibition of triple-negative and herceptin-resistant breast cancer cell proliferation and migration by annexin A2 antibodies. Br. J. Cancer, 111: 2328-2341.
21. Wu, P.C., J.W. Lu, J.Y. Yang, I.H. Lin and D.L. Ou *et al*., 2014. H3K9 histone methyltransferase, KMT1E/SETDB1, cooperates with the SMAD2/3 pathway to suppress lung cancer metastasis. Cancer Res., 74: 7333-7343.
22. Zhang, Z.D., Y. Li, L.Q. Fan, Q. Zhao, B.B. Tan and X.F. Zhao, 2014. Annexin A2 is implicated in multi-drug-resistance in gastric cancer through p38MAPK and AKT pathway. Neoplasma, 61: 627-637.
23. Jung, H., J.S. Kim, W.K. Kim, K.J. Oh and J.M. Kim *et al*., 2015. Intracellular annexin A2 regulates NF-κB signaling by binding to the p50 subunit: Implications for gemcitabine resistance in pancreatic cancer. Cell Death Dis., Vol. 6. 10.1038/cddis.2014.558.
24. Zhai, H., S. Acharya, I. Gravanis, S. Mehmood and R.J. Seidman *et al*., 2011. Annexin A2 promotes glioma cell invasion and tumor progression. J. Neurosci., 31: 14346-14360.
25. Baron, A., M. Mancini, E. Caldwell, A. Cabrelle, P. Bernardi and F. Pagano, 2009. *Serenoa repens* extract targets mitochondria and activates the intrinsic apoptotic pathway in human prostate cancer cells. BJU Int., 103: 1275-1283.
26. Zhou, T., Y. Yang, H. Zhang, Y. Che and W. Wang *et al*., 2015. *Serenoa repens* induces growth arrest, apoptosis and inactivation of STAT3 signaling in human glioma cells. Technol. Cancer Res. Treat., 14: 729-736.
27. González-Arenas, A., M.D. la Fuente-Granada, I. Camacho-Arroyo, C.J. Zamora-Sánchez, A.G. Piña-Medina, J. Segura-Uribe and C. Guerra-Araiza, 2019. Tibolone effects on human glioblastoma cell lines. Arch. Med. Res., 50: 187-196.
28. Vinarov, A.Z., L.G. Spivak, D.V. Platonova, L.M. Rapoport and D.O. Korolev, 2019. 15 years' survey of safety and efficacy of *Serenoa repens* extract in benign prostatic hyperpl Asia patients with risk of progression. Urologia J., 86: 17-22.
29. Yang, Y., L. Hui, C. Yuqin, L. Jie, H. Shuai, Z. Tiezhu and W. Wei, 2014. Effect of saw palmetto extract on PI3K cell signaling transduction in human glioma. Exp. Ther. Med., 8: 563-566.

30. Romani, M., M.P. Pistillo, R. Carosio, A. Morabito and B. Banelli, 2018. Immune checkpoints and innovative therapies in glioblastoma. Front. Oncol., Vol. 8. 10.3389/fonc.2018.00464.
31. Krasnikova, T.L., T.I. Arefieva, E.A. Pylaeva and M.V. Sidorova, 2016. Ingramon, a peptide inhibitor of MCP-1 chemokine, reduces migration of blood monocytes stimulated by glioma-conditioned medium. Bull. Exp. Biol. Med., 160: 480-482.
32. Platten, M., A. Kretz, U. Naumann, S. Aulwurm, K. Egashira, S. Isenmann and M. Weller, 2003. Monocyte chemoattractant protein-1 increases microglial infiltration and aggressiveness of gliomas. Ann. Neurol., 54: 388-392.
33. Zhu, X., M. Fujita, L.A. Snyder and H. Okada, 2011. Systemic delivery of neutralizing antibody targeting CCL2 for glioma therapy. J. Neuro-Oncol., 104: 83-92.
34. Lindemann, C., V. Marschall, A. Weigert, T. Klingebiel and S. Fulda, 2015. Smac mimetic-induced upregulation of CCL2/MCP-1 triggers migration and invasion of glioblastoma cells and influences the tumor microenvironment in a paracrine manner. Neoplasia, 17: 481-489.
35. Mattila, S., H. Tuominen, J. Koivukangas and F. Stenbäck, 2009. The terminal prostaglandin synthases mPGES-1, mPGES-2 and cPGES are all over expressed in human gliomas. Neuropathology, 29: 156-165.
36. Silvestri, I., S. Cattarino, A. Aglianò, C. Nicolazzo and S. Scarpa *et al*., 2013. Effect of *Serenoa repens* (Permixon®) on the expression of inflammation-related genes: Analysis in primary cell cultures of human prostate carcinoma. J. Inflammation, Vol. 10. 10.1186/1476-9255-10-11.
37. Latil, A., C. Libon, M. Templier, D. Junquero, F. Lantoine-Adam and T. Nguyen, 2012. Hexanic lipidosterolic extract of *Serenoa repens* inhibits the expression of two key inflammatory mediators, MCP-1/CCL2 and VCAM-1, *In vitro*. BJU Int., 110: E301-E307.
38. Goldmann, W.H., A.L. Sharma, S.J. Currier, P.D. Johnston, A. Rana and C.P. Sharma, 2001. Saw palmetto berry extract inhibits cell growth and Cox-2 expression in prostatic cancer cells. Cell Biol. Int., 25: 1117-1124.